# RECOILING BLACK HOLES IN STATIC AND EVOLVING DARK MATTER HALO POTENTIAL

**M. Smole**

*Astronomical Observatory, Volgina 7, 11060 Belgrade 38, Serbia*

E–mail: *msmole@aob.rs*

SUMMARY: We follow trajectories of kicked black holes in static and evolving dark matter halo potential. We explore both NFW and Einasto dark matter density distributions. The considered dark matter halos represent hosts of massive spiral and elliptical field galaxies. We study the critical amplitude of kick velocity necessary for complete black hole ejection at various redshifts and find that $\sim 40\%$ lower kick velocities can remove black holes from their host haloes at $z = 7$ compared to $z = 1$. The greatest difference between the static and evolving potential occurs near the critical velocity for black hole ejection and at high redshifts. When NFW and Einasto density distributions are compared $\sim 30\%$ higher kick velocities are needed for complete removal of BHs from dark matter halo described by the NFW profile.

Key words. dark matter – galaxies: halos – black hole physics – gravitational waves

## 1. INTRODUCTION

According to the currently favoured hierarchical growth of structure, dark matter (DM) haloes and the associated galaxies experience multiple mergers during their history. Black holes (BHs) in their centres form a binary system due to dynamical friction. Further binary hardening requires stellar dynamical processes. BH binaries capture nearby stars and then eject them at much higher velocities. This tree-body interactions carry away energy of the system and decrease the separation between BHs (Begelman et al. 1980). When BHs get close enough, the energy losses due to gravitational radiation cause them to merge. If the merging BHs have unequal masses or spins the asymmetric emission of gravitational radiation can lead to BH kick. Gravitational waves propagate in a preferential direction due to non-zero net linear momentum and the centre of mass of the binary recoils in the opposite direction (Redmount and Rees 1989).

Gravitational wave recoil can displace a newly formed BH from the galaxy core or completely eject it if the BH speed is larger than the escape velocity from the halo centre. The magnitude of the gravitational wave recoil depends on the mass ratio of BHs, the spin magnitude and orientation with respect to the binary orbital plane, and the eccentricity of the orbit (e.g. Schnittman and Buonanno 2007, Baker et al. 2002). Both analytic and numerical calculations show that maximum recoil velocity for non spinning BHs is < 200 km/s (Fitchett and Detweiler 1984, Favata et al. 2004, Blanchet et al. 2005, Damour and Gopakumar 2006, Baker et al. 2006, Gonzalez et al. 2007b). Similar values are expected for BHs with low spins or with spins aligned with the binary orbital angular momentum. Calculations using the perturbation theory suggested that kick velocities should not to exceed 500 km/s (Favata et al. 2004). However, full numerical relativity simula-

tions have shown that when the spin vectors have opposite directions and are in the orbital plane, the recoil velocity can be as large as $\sim 4000$ km/s (Herrmann et al. 2007, Gonzales et al. 2007a, 2007b, Campanelli et al. 2007a, 2007b, Schnittman and Buonanno 2007, Koppitz et al. 2007). Lousto and Zlochower (2011) suggested that the kick velocity could approach 5000 km/s for spins partially aligned with the orbital angular momentum.

Such large velocities are able to eject BH even from massive elliptical galaxies whose escape velocity is $\sim 3000$ km/s (Merritt et al. 2004). On the other hand, much lower kick velocities ($\sim 200$ km/s) can eject BHs from globular clusters or low mass galaxies. Also, DM haloes at high redshifts have low masses and thus shallow potential wells so that kick velocities of $\sim 150$ km/s can be sufficient to eject BHs from the centre of the most massive haloes at redshift $z \geq 11$ (Merritt et al. 2004, Micic et al. 2006, Volonteri 2007, Schnittman 2007, Sesana 2007, Volonteri et al. 2010, Micic et al. 2011).

Gravitational wave recoil can significantly affect the SMBH growth through mergers. Pop III stars are believed to form early, at $z \sim 20$, and leave BH seeds with typical masses of $\sim 100\ M_\odot$. Those BH seeds could merge to form SMBHs observed in high redshift quasars (Madau and Rees 2001, Heger et al. 2003, Wise and Abel 2005). However, the BHs at high redshift haloes with shallow potential wells might be very sensitive to gravitational wave recoil and thus the BH growth can be suppressed (e.g. Haiman 2004, Merritt et al. 2004, Volonteri 2007).

If the kick velocity is lower than the escape velocity of the host BH will gradually return to the halo centre due to dynamical friction against stars and gas. Several authors calculated the trajectories of recoiling BHs in a purely stellar systems (e.g. Madau and Quataert 2004, Boylan-Kolchin et al. 2004, Gualandris and Merritt 2008). After reaching the maximum distance, a BH in such systems makes several passages across the centre of the galaxy and sinks back to the core. The time scale for orbit decay depends on the kick velocity and surrounding density. Gualandris and Merritt (2008) have shown that a BH which returns to the core exhibits long-lived oscillations with amplitude comparable to the core radius which can last 1 Gyr in the case of massive galaxies. A kicked BH transfers kinetic energy to the stars which lower the core density (Redmount and Rees 1989, Merritt et al. 2004, Boylan-Kolchin et al. 2004). BH trajectories in a potential that includes both the stellar bulge and gaseous disk have also been studied numerically (Devecchi et al. 2009, Blecha et al. 2011, Guedes et al. 2011, Sijacki et al. 2011). Gas content of galaxies has a high influence on recoiling BH trajectories. BH will spent significantly less time wandering in the gas-rich galaxy than in the gas-poor galaxy (Blecha et al. 2011). Guedes et al. (2011) and Sijacki et al. (2011) suggested that in gas-rich major merger remnants, BHs should only rarely be able to escape from massive galaxies at high redshifts due to the presence of a massive gaseous disc. Vicari et

al. (2007) have shown that time scales for orbital decay of BHs kicked from triaxial potential are longer than in spherical potential since a recoiling BH does not return directly through the dense centre where the dynamical friction force is highest.

Several authors suggested that, since the typical recoiling velocity is smaller than the escape velocity of the Milky Way halo, many 'rogue' BHs should remain in the halo today (Volonteri and Perna 2005, Libeskind et al. 2006, O'Leary and Loeb 2009, 2011, Micic et al. 2011).

Recoiling BHs could leave observable signatures. Ejected BHs carry an accretion disk, which can be observed as spatially or kinematically offset quasars (e.g. Madau and Quataert 2004, Loeb 2007, Blecha and Loeb 2008, Blecha et al. 2011, Guedes et al. 2011, Sijacki et al. 2011). In the case of a spatially-offset AGN, the accreting BH is displaced from the host's nucleus while in the case of kinematically-offset AGN, the broad line region carried by the recoiling BH is displaced by a velocity $\Delta v$ from the narrow line region associated with the host galaxy. Blecha and Loeb (2008) suggested that finding such quasars could be challenging. Large kick velocities result is large offsets but those BHs have small accretion disk and thus short quasar lifetime. On the other hand, low kick velocities imply short wandering time. However, when a supply of bound gas is exhausted a BH can again become active while passing through the galactic gas disk. These passes would produce knotted or twisted jets. Non-active recoiling BH could be observed through the imprint on the gaseous medium of the host galaxy (Devecchi et al. 2009). Guedes et al. (2011) showed that changes in the central density profile are significant only in the case of minor mergers. A SMBH binary could also explain precessing jets and X-shaped sources observed in some radio sources (e.g. Merritt and Ekers 2002, Zier 2005).

Most of the above works followed trajectories of recoiling BHs in a static potential and neglected the impact of galaxy evolution.

DM haloes and galaxies grow by smooth accretion from the cosmic web and through mergers. There are two types of accretion: the hot accretion, where hot, virialised gas in halo cools, loses its pressure support and settles into a disk (Rees and Ostriker 1977, White and Rees 1978, Fall and Efstathiou 1980), and the cold accretion through dark matter filaments (Dekel and Birnboim 2006). The hot accretion dominates the growth of massive galaxies in galaxy clusters at low redshifts, while cold accretion dominates in lower mass structures and at high redshifts.

Spiral galaxies formed first and they grew mainly through the cold mode accretion. In high density regions of space, large number of mergers lead to formation of galaxy clusters. The most massive galaxies reside in clusters where they can grow both by mergers (which are common because of the high density environment) and by accretion of the shock heated gas (hot accretion). Elliptical galaxies are formed by major mergers of gas-rich spiral galaxies and they continue to grow by continuous in-

fall of dwarf galaxies, the so called minor mergers. The fraction of elliptical galaxies in galaxy clusters is high compared to the field. In less dense regions field galaxies grows in isolation, mergers are rare and cold accretion dominates (Micic 2013 and references therein).

The goal of this paper is to compare trajectories of recoiling BHs in a static and evolving DM potential. The evolving DM potential is calculated using the van den Bosch et al. (2014) code. We focus on two dark matter haloes: one with mass of $10^{12} M_\odot$ which represents a Milky Way-type host and the other with mass of $2 \times 10^{13} M_\odot$ which is the host of the most massive field elliptical galaxy (Niemi et al. 2010). Considered DM haloes have masses which correspond to hosts of a typical and the most massive field galaxies as well as the group of galaxies in the field at $z < 1$. The same halo masses are also typical of the proto-cluster environment at higher redshifts. This chosen mass interval is of the greatest significance for studying the effects of BH kicks on SMBH population in massive galaxies because, once the cluster is formed, deep gravitational well in cluster prevents a recoiling BH to be completely ejected. Since both galaxies are isolated it can be assumed that the halo growth is due to the cold mode accretion and that mergers can be neglected.

Recent N-body simulations (Navarro et al. 2004, 2010, Merritt et al. 2006, Gao et al. 2008, Hayashi and White 2008, Stadel et al. 2009, Reed et al. 2011, Dutton and Macciò 2014) have shown that DM haloes are better described by Einasto profile (1965) than by the NFW profile (Navarro et al. 1997). NFW and the Einasto models differ mainly at small radii ($\sim 1\%$ of the virial radius) where the Einasto profile implies lower density. In this paper we consider both the NFW and Einasto DM density distributions.

In Section 2 we describe the method. The results are presented in Section 3. We summarise and discuss the results in Section 4.

## 2. METHOD

In this paper we follow trajectories of recoiling BHs in a DM halo which is distributed according to a NFW profile (Navarro et al. 1997) and the Einasto profile (Einasto 1965). A BH is placed at the halo's centre and kicked with recoil velocity $v_{kick}$ at redshift $z_{kick}$. Its orbit is then governed by the potential of a NFW/Einasto density distribution. Two different cases are explored: The BH orbits in a static, and in evolving potential. At multiple runs, various kick velocities are assigned to BHs at different redshifts in both a static and evolving potential.

The amplitude of the kick determines whether the BH will be removed from its host or not. If the escape velocity is greater than the kick velocity, a BH will return to the halo centre. Dynamical friction against stars (e.g. Merritt et al. 2004, Madau and Quataert 2004, Boylan-Kolchin et al. 2004, Gualandris and Merritt 2008) and gas (e.g. Blecha et al. 2011, Guedes et al. 2011, Sijacki et al. 2011) leads

to the orbit decay and, after several passages across the galaxy centre, the BH will settle down in the bottom of potential well. In this paper, since BH trajectories are followed in pure DM halo potential, it is assumed that each BH which passed across the halo's centre stayed there due to dynamical friction which acts as to slow the BH down.

We consider two DM haloes. The first one has mass of $10^{12} M_\odot$ at redshift $z = 0$ (Halo 1 in further text) and it represents a Milky Way-type host. The second DM halo with mass of $2 \times 10^{13} M_\odot$ (Halo 2) hosts the most massive field elliptical galaxy (Niemi et al. 2010).

### 2.1. Evolving potential

The evolving NFW density profile is modeled using a code given by van den Bosch et al. (2014)[1]. Van den Bosch et al. (2014) have studied the growth of DM haloes which can be characterised by its mass accretion history (MAH) and the potential well growth history (PWGH). They follow the growth of DM haloes described by an NFW density profile:

$$\rho_{NFW}(r) = \rho_{crit} \frac{\delta_{char}}{r/r_s \left(1 + r/r_s\right)^2} \qquad (1)$$

where $\rho_{crit} = 3H^2(z)/8\pi G$ is the critical density for closure, $r_s$ is the scale radius and $\delta_{char}$ is defined as

$$\delta_{char} = \frac{\Delta_{vir}}{3} \frac{c^3}{f(c)}, \qquad (2)$$

with $c = r_{vir}/r_s$ the halo concentration parameter:

$$f(x) = \ln(1 + x) - \frac{x}{1 + x}, \qquad (3)$$

and:

$$\Delta_{vir}(z) = 18\pi^2 + 82x - 39x^2, \qquad (4)$$

where $x = \Omega_z - 1$.

The maximum circular velocity, which occurs at radius $r_{max} \simeq 2.16\, r_s$, is given by:

$$V_{max} = 0.465\, V_{vir} \sqrt{\frac{c}{f(c)}}. \qquad (5)$$

The virial velocity, defined as the circular velocity at the virial radius, is:

$$V_{vir} = 159.43 \text{km/s} \left(\frac{M}{10^{12} h^{-1} M_\odot}\right)^{1/3} \left[\frac{H(z)}{H_0}\right]^{1/3} \left[\frac{\Delta_{vir}(z)}{178}\right]^{1/6}. \qquad (6)$$

The authors use the model for halo concentration from Zhao et al. (2009):

$$c(M, t) = c(t, t_{0.04}) = 4.0 \left[1 + \left(\frac{t}{3.75\, t_{0.04}}\right)^{8.4}\right]^{1/8}, \qquad (7)$$

where $t_{0.04}$ is the proper time at which the host halo's main progenitor gained 4 percent of its mass. The gravitational potential of a spherical NFW density distribution is given by:

$$\Phi(r) = -V_{\mathrm{vir}}^2 \frac{\ln(1 + cx)}{f(c)\, x} = -\left(\frac{V_{\max}}{0.465}\right)^2 \frac{\ln(1+cx)}{cx},$$
(8)

where $x = r/r_{\mathrm{vir}}$. This method is described in Jiang and van den Bosch (2014). Since the halo's gravitational potential is directly proportional to the square of the maximum circular velocity $V_{\max}$, it can be used to track halo's growth history.

The authors use the extended Press-Schechter (EPS) formalism (Bond et al. 1991) to make merger trees from which they determine the MAH. For a halo with a given mass at the final redshift they trace the merger tree to determine the mass of its main progenitor as function of redshift. Next, they use the mass of the main progenitor to compute the maximum circular velocity (Eqs. 5 and 6). Hence, the extracted MAH $(M(z)/M_0)$ is used for computing PWGH $(V_{\max}(z)/V_{\mathrm{vir},0})$. The authors test and calibrate their model using merger trees from the Bolshoi simulation (Klypin et al. 2011).

They found that MAHs have a universal form which they use to compute the average MAH and PWGH for a halo of any mass in any $\Lambda$CDM cosmology.

## 2.2. Static potential

The potential of a DM halo which follows the NFW density distribution (Eq. 1) is given by:

$$\Phi_{\mathrm{NFW}}(r) = -4\pi G \delta_{\mathrm{char}} \rho_{\mathrm{crit}} r_{\mathrm{s}}^2 \left(\frac{r_{\mathrm{s}}}{r}\right) \ln\left(\frac{r + r_{\mathrm{s}}}{r_{\mathrm{s}}}\right),$$
(9)

where parameters $\delta_{\mathrm{char}}$, $\rho_{\mathrm{crit}}$ and $r_{\mathrm{s}}$ are defined in Section 2.1.

The Einasto density distribution (Einasto 1965) is

$$\rho_{\mathrm{Ein}}(r) = \rho_{-2} \exp\left\{-\frac{2}{\alpha}[(r/r_{-2})^\alpha - 1]\right\},$$
(10)

where $r_{-2}$ is the radius where the logarithmic slope of the density profile is equal to -2, analogous to the $r_s$ of a NFW profile, $\rho_{-2}$ is the density at that radius and $\alpha$ is a parameter that describes the shape of the density profile. The potential of DM distributed according to the Einasto model is given by Cardone et al. (2005):

$$\Phi_{\mathrm{Ein}}(x) = -\frac{GM_{\mathrm{tot}}}{r_{-2}} \mathcal{F}(x; \alpha),$$
(11)

with:

$$\mathcal{F}(x; \alpha) = \frac{\Gamma(3/\alpha) - \Gamma(3/\alpha, 2x^\alpha/\alpha)}{x\Gamma(3/\alpha)} +$$
$$\left(\frac{2}{\alpha}\right)^{1/\alpha} \frac{\Gamma(2/\alpha) + \Gamma(2/\alpha, 2x^\alpha/\alpha)}{\Gamma(3/\alpha)}$$
(12)

where $x$ is defined as $x \equiv r/r_{-2}$, $M_{\mathrm{tot}}$ is the total mass of the DM halo and $\Gamma(x)$ and $\Gamma(a, x)$ are the $\Gamma$ function and the incomplete $\Gamma$ function, respectively.

The Einasto profile has an additional shape parameter $\alpha$ whose value is mass dependent. $\alpha$ increases with halo mass and redshift with $\alpha \sim 0.16$ for galaxy size haloes and $\alpha \sim 0.3$ for the most massive clusters (e.g. Navarro et al. 2004, 2010, Gao et al. 2008, Hayashi and White 2008, Dutton and Macciò 2014). This implies that DM haloes are not strictly universal as suggested by the NFW profile which has a fixed shape and mass and size as two scaling parameters.

## 2.3. Recoiling BH in evolving potential

The code given by van den Bosch et al. (2014) is designed to compute the average MAH and PWGH. Input parameters are the final redshift, final DM halo mass, and cosmology. The $\Lambda$CDM cosmology used in this paper is:

$$\Omega_{\mathrm{m}} = 0.27, \, \Omega_\Lambda = 0.73, \, h = 0.7, \, \sigma_8 = 0.8, \, n_s = 0.95,$$

where $h$ is the Hubble constant at $z = 0$ in units of 100 km s$^{-1}$ Mpc$^{-1}$, $\sigma_8$ is the rms amplitude of linear mass fluctuations in $8h^{-1}$ Mpc spheres at $z = 0$, and $n_{\mathrm{s}}$ is the spectral index of the primordial power spectrum.

Using this code we compute growth of two DM haloes. DM halo masses at $z = 0$ are chosen to be $10^{12} M_\odot$ (Halo 1) and $2 \times 10^{13} M_\odot$ (Halo 2). Halo parameters at $z = 0$ (the code output) are $c = 9.9$ and $r_{\mathrm{s}} = 24.5$ kpc for Halo 1 and $c = 7.4$ and $r_{\mathrm{s}} = 88.7$ kpc for Halo 2.

Next step is to integrate the trajectory of the BH under the influence of evolving potential described by Eq. 8. Variables in Eq. 8 are the maximum circular velocity and halo concentration parameter, and both parameters are the output of the code. The BH is placed at halo's centre at $z_{\mathrm{kick}} > 0$ and kicked by the recoil velocity $v_{\mathrm{kick}}$. We follow the evolution of the parent halo from $z = 7$ to $z = 0$. At each time-step the halo potential is modified, and BH's position and velocity is updated. At multiple runs, different kick velocities are assigned to the BH at different redshifts so that the entire parameter space is explored.

To calculate BH trajectories in the evolving Einasto potential we assume that the choosing different density distributions (NFW or Einasto) does not change the total halo mass at the given redshift, so we can use the MAH calculated by the van den Bosch et al. (2014) code. We follow recoiling BHs in the potential described by Eq. 11 and, as in the case of evolving NFW profile, at each time-step the halo potential is modified and BH's position and velocity are updated. The evolution of parameter $\alpha$ is taken from Dutton and Macciò (2014). In their Fig. 13 the authors show how the Einasto shape parameter varies with halo mass for a range of different redshifts $(0 < z < 5)$. We follow BHs in evolving Einasto potential from $z = 5$ to $z = 0$.

## 2.4. Recoiling BH in static potential

We repeat the same procedure for a BH kicked from the centre of a halo whose potential is static and described with the NFW/Einasto density distribution. Static NFW and Einasto density profiles have the same halo parameters as the evolving NFW/Einasto profile at redshift $z = 0$ ($10^{12}\,M_\odot$ and $r_{\rm s} = 24.5$ kpc for Halo 1, and $2 \times 10^{13}\,M_\odot$ and $r_{\rm s} = 88.7$ kpc for Halo 2). The Einasto shape parameter is taken to be $\alpha = 0.16$ which is the expected value for a galaxy size halo at redshift $z = 0$ (e.g. Dutton and Macciò 2014). Again, the BH is kicked from the halo's centre but this time, since the potential is static, only the BH's position and velocity is updated at each time-step. We integrate BHs trajectories under the influence of DM potentials given by Eqs. 9 (NFW) and 11 (Einasto) for ranges of $z_{\rm kick}$ and $v_{\rm kick}$.

We compare the BH's position at redshift $z = 0$ in a static and evolving potential to see how the host halo's evolution and mass growth affect orbits of recoiling BHs for both NFW and Einasto density distributions.

## 3. RESULTS

Fig. 1 shows evolution of two DM haloes considered in this paper. The DM halo growth history is the output of the code taken from van den Bosch et al. (2014). The black solid line corresponds to the mass growth of Halo 1, while the blue dashed line represents Halo 2. The considered haloes grow in isolation so the growth is dominated by smooth cold mode accretion from the cosmic web.
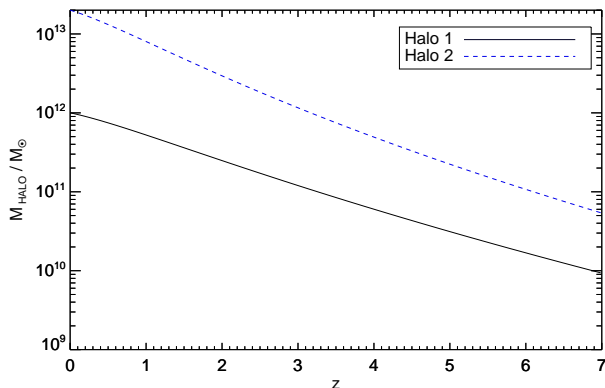


**Fig. 1.** *Halo mass as a function of redshift. The growth history is taken from van den Bosch et al. (2014). The black solid and blue dashed lines represent evolution of Halo 1 and Halo 2, respectively.*

Fig. 2 shows displacement of a kicked BH from a host halo's centre at $z = 0$ as a function of $v_{\rm kick}$ and $z_{\rm kick}$. BH trajectories are calculated in the evolving and static potential for both NFW (right) and Einasto (left) density distributions for Halo 1 (top

panels) and for Halo 2 (bottom panels). White lines represent the critical velocity for complete BH ejection.

In the case of a static NFW potential, the gravitational well is deep even at high redshifts and moderate kick velocities cannot eject the BH from the host halo. BHs kicked from the centre of Halo 1 (Halo 2) will return to the bottom of the potential well if $v_{\rm kick} \leq 500$ km/s ($v_{\rm kick} \leq 1350$ km/s), independent of $z_{\rm kick}$. The critical velocity for ejection of a BH from Halo 1 (Halo 2) described by the static Einasto profile is $v_{\rm kick} \sim 370$ km/s ($v_{\rm kick} \sim 850$ km/s).

On the other hand, Fig 1. shows that haloes grow by approximately two orders of magnitude from $z = 7$ to $z = 0$. If this evolution is taken into account, haloes at high redshifts have relativity low masses compared to the static case and the BH displacement is more sensitive to $z_{\rm kick}$. Amplitude of a kick necessary to remove the BH from Halo 1 (Halo 2) varies from 300 km/s (725 km/s) at $z = 7$ to 500 km/s (1200 km/s) at $z = 1$ in the case of evolving NFW potential, and from 200 km/s (350 km/s) at $z = 5$ to 280 km/s (600 km/s) at $z = 1$ in the case of evolving Einasto potential.

The critical velocity for a complete BH ejection is $\sim 30\%$ lower for the static Einasto profile than for the static NFW profile, and $\sim 50\%$ lower when the evolving Einasto and NFW profiles are compared. For a given DM halo mass the Einasto and NFW distributions differ at small radii where the Einasto profile predicts a shallower potential well and thus a lower escape velocity.

Note that Fig 2. shows a sharp edge between BHs that return back to the bottom of the potential well and BHs whose displacement is $\sim 1$Mpc. This is a consequence of using a pure DM potential. Usually one expects a greater number of rogue BHs wondering in the galaxy's halo (Volonteri and Perna 2005, Libeskind et al. 2006, O'Leary and Loeb 2009, 2011, Micic et al. 2011). If amplitude of the kick is not large enough to completely eject the BH, BH will cross the galaxy core several times before it settles down. In the dense centre, dynamical friction force is highest and BH's orbits decay. However, in this paper, only the DM halo is considered and there are no interactions with stars and gas which can slow down the recoiling BH. Because of that, it is assumed that each BH that reaches the galaxy core stays there.

In Fig. 3 we compare positions of recoiling BHs in a static and evolving NFW/Einasto potentials. Fig. 3 shows the difference between the distance from the galaxy's core that a BH can reach at $z = 0$ for a static and evolving potential, as a function of $v_{\rm kick}$ and $z_{\rm kick}$. Upper panels represent Halo 1 while bottom panels represent Halo 2.

Both haloes show the greatest differences at high redshifts where the evolving DM halo has low mass and thus shallow potential well. Also, the greatest deviation occurs near the critical velocity needed for complete ejection of a BH from the static potential.
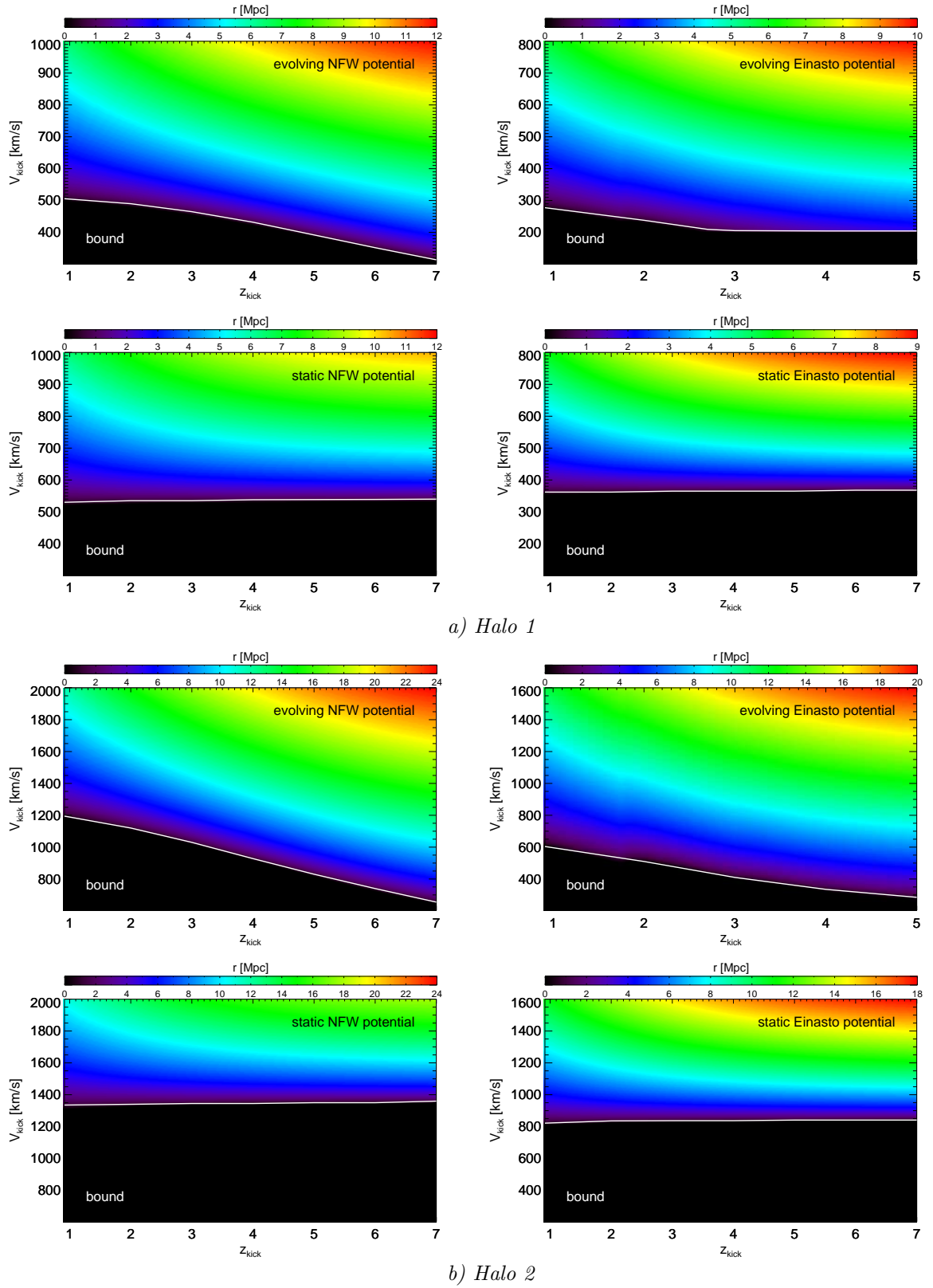
*a) Halo 1*

*b) Halo 2*

**Fig. 2.** *Distance of a kicked BH from a host halo's centre at z=0 as a function of $v_{kick}$ and $z_{kick}$. Top panels represent evolving and static NFW (right)/Einasto (left) potential for Halo 1 and bottom panels correspond to Halo 2. White lines represent critical velocity for complete BH ejection. Distance of a kicked BH from a host halo's centre, r[Mpc], is represented by different colours.*
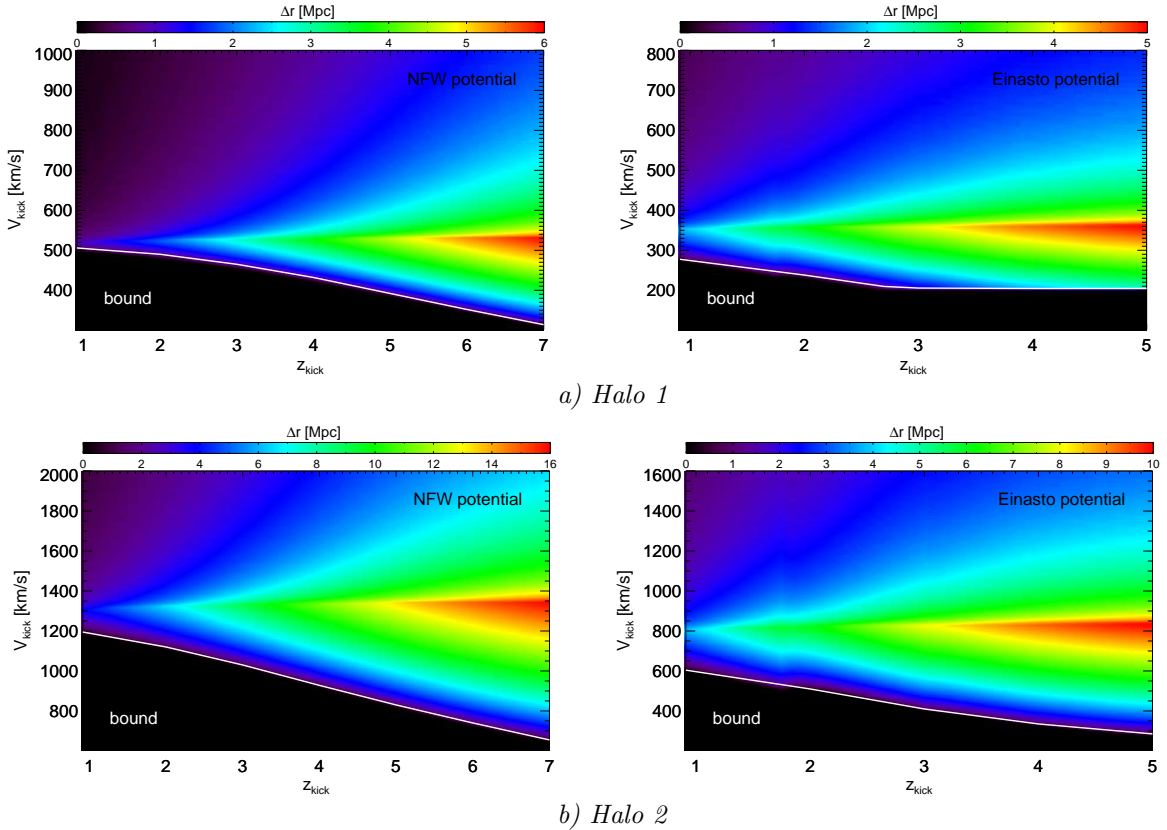
a) Halo 1



b) Halo 2

**Fig. 3.** *Difference between the distance of a kicked BH from a host halo's centre at z=0 in the case of static and evolving NFW/Einasto potential as a function of $v_{\text{kick}}$ and $z_{\text{kick}}$. Top panels represent Halo 1 while bottom panels represent Halo 2. White lines represent the critical velocity below which BHs will stay in the host halo for both static and evolving case. The difference between BH positions in static and evolving potential, $\Delta r[\text{Mpc}]$, is represented by different colours.*

Black region in Fig. 3 represents the parameter space where a recoiling BH will stay in its host halo for both the static and evolving cases. For these values of $v_{\text{kick}}$ and $z_{\text{kick}}$ host halo evolution does not effect BH's position at $z = 0$. White lines in Fig 3. represent minimum values of $v_{\text{kick}}$ necessary to remove the BH from the evolving potential halo for a given value of $z_{\text{kick}}$.

Fig. 4 shows the distance from the host's centre at $z = 0$ as a function of $v_{\text{kick}}$ for four different kick redshifts ($z_{\text{kick}} = 1, 3, 5, 7$). At higher redshifts kick, amplitude in the evolving potential has a greater impact on the final BH distance. At $z = 1$ the evolving potential does not significantly differ from the static potential and the final BH positions are similar for both cases. The difference between the static and evolving potentials is more pronounced for Halo 2 which has greater mass. The same behaviour is noticeable for both NFW and Einasto density distributions.

The difference between a static and evolving potentials can be represented in the form:

$$v_{\text{kick,evol}} = \frac{v_{\text{kick,stat}}}{f(z)} \qquad (13)$$

where $v_{\text{kick,evol}}$ and $v_{\text{kick,stat}}$ are minimum values of the kick amplitude necessary to remove BH from the host halo for evolving and static potentials, respectively, and $f(z)$ is the fitting function. Fitting function is a quadratic polynomial with coefficients:

$$f(z)_{\text{Halo1(Halo2)}} = 0.01(0.02)z^2 - 0.01(-0.03)z \\ +1.05(1.07) \quad (14)$$

for the NFW profile, and:

$$f(z)_{\text{Halo1(Halo2)}} = -0.05(-0.03)z^2 + 0.42(0.23)z \\ +0.92(1.08) \quad (15)$$
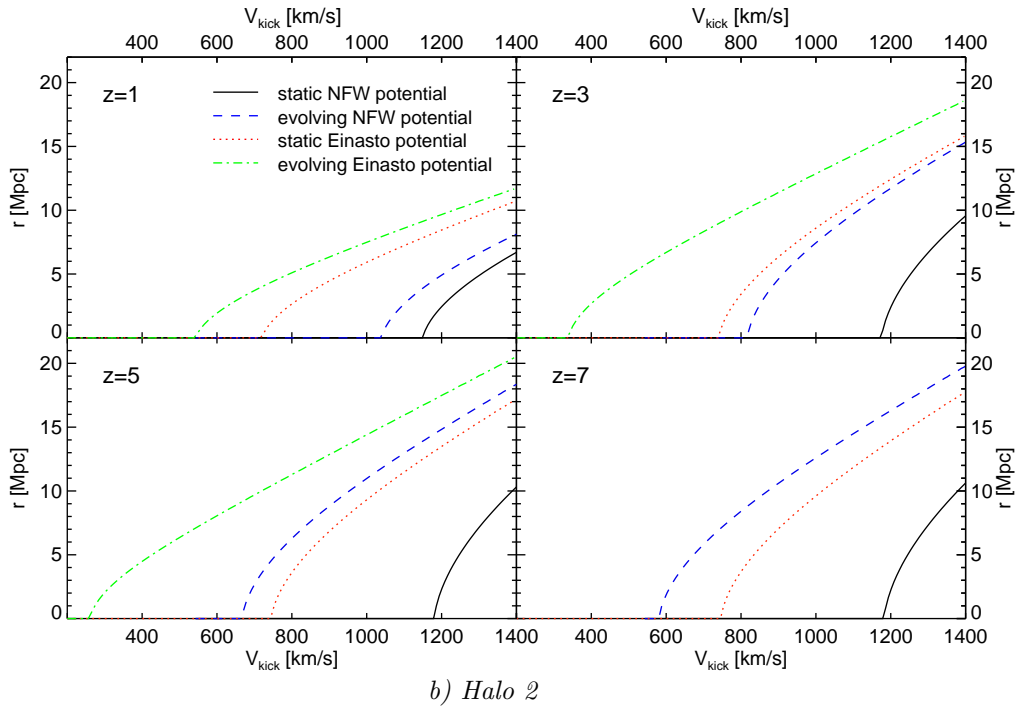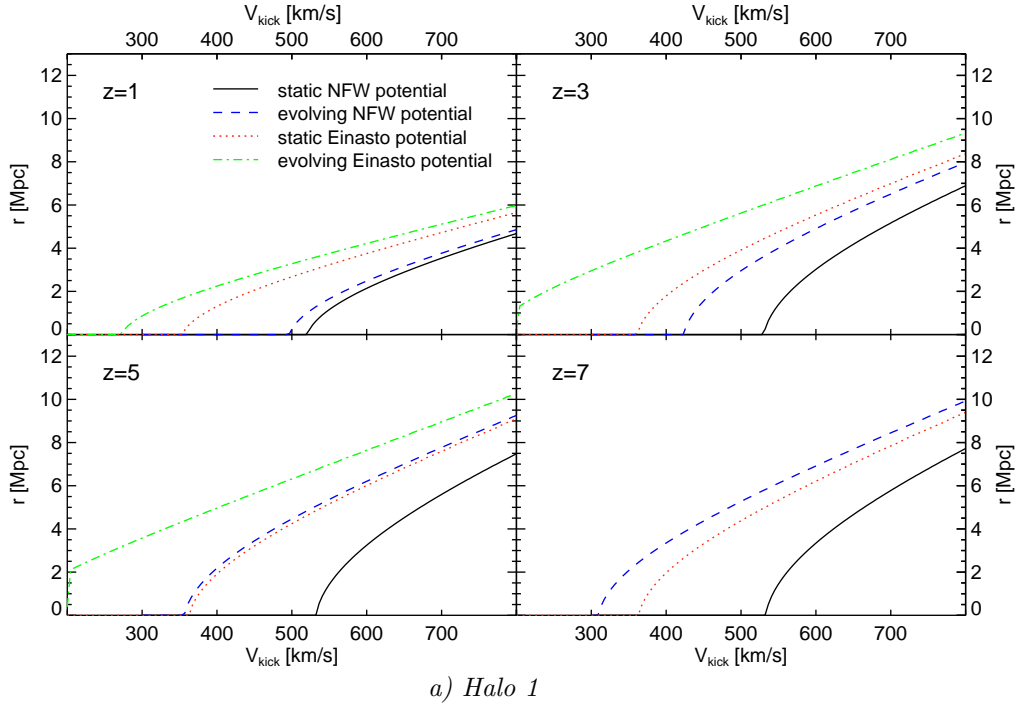
for the Einasto profile.

23

a) Halo 1



b) Halo 2

**Fig. 4.** *Distance of a recoiling BH from halo's centre at z=0. The upper panel shows Halo 1 while the bottom panel shows Halo 2.*

## 4. DISCUSSION

In this paper, trajectories of kicked BHs are followed in static and evolving DM halo potentials described by the NFW and Einasto density distributions. Growth and evolution of DM haloes are calculated using the van den Bosch et al. (2014) code. DM haloes considered in this paper have masses $10^{12}\,M_\odot$ (Halo 1) and $2 \times 10^{13}\,M_\odot$ (Halo 2) at $z = 0$. These haloes represent hosts of a Milky Way-type galaxy and the most massive field elliptical galaxy (Niemi et al. 2010), respectively. BHs are placed in the halo's centre and given various kick velocities at various redshifts, so the entire parameter space is explored. BH positions at redshift $z = 0$ are compared for static and evolving potentials for both NFW and Einasto density profiles.

When a BH is kicked from the center of a static NFW potential, the gravitational well is deep even at high redshifts. The critical kick velocity necessary for a complete BH ejection varies from $v_{\mathrm{kick}} \sim 500$ km/s for a Milky Way-type host to $v_{\mathrm{kick}} \sim 1350$ km/s for a massive elliptical field galaxy, and it is constant with redshift. If a shallower Einasto potential is adopted, then critical velocities are lower: $v_{\mathrm{kick}} \sim 370$ km/s for a Milky Way size halo and $v_{\mathrm{kick}} \sim 850$ km/s for an elliptical galaxy.

However, if the host halo evolves then the critical velocity for ejection is sensitive to redshift at which the BH is kicked. To remove the BH from its host at redshift $z = 0$, kick velocity needs to have $\sim 40\%$ larger amplitude at $z_{\mathrm{kick}} = 1$ compared to $z_{\mathrm{kick}} = 7$ for both Milky Way and massive elliptical type hosts. In evolving NFW potential, critical velocity varies from 300 km/s at $z_{\mathrm{kick}} = 7$ to 500 km/s at $z_{\mathrm{kick}} = 1$ for Halo 1, and from 725 km/s at $z_{\mathrm{kick}} = 7$ to 1200 km/s at $z_{\mathrm{kick}} = 1$ for Halo 2. Again, if the evolving Einasto potential is considered, then the critical velocities are lower: 200(350) km/s at $z_{\mathrm{kick}} = 5$, and 280(600) km/s at $z_{\mathrm{kick}} = 1$ for Halo 1 and Halo 2, respectively.

When static and evolving potentials are compared, the BH positions at redshift $z = 0$ show the greatest difference near the critical velocity and at high redshifts. This applies to both considered haloes and both density distributions. At high redshifts, evolving haloes have shallow potential wells and kick amplitude has a greater impact on the final BH position.

The gravitation wave recoil can affect the SMBH growth since ejected BHs are less likely to merge with other BHs. The question that remains is how often BHs get significant kick velocities. As summarised by Blecha and Loeb (2008), several authors have calculated kick distributions. Schnittman and Buonanno (2007), Campanelli et al. (2007a) and Baker et al. (2008) found that 12, 36, and 23 per cent of recoiling BHs have velocities > 500 km/s, and 3, 13, and 9 per cent have > 1000 km/s, respectively. This is calculated under the assumption that BH spins are $a = 0.9$ and that BH mass ratios are within the range $1/10 \leq m_1/m_2 \leq 1$.

In the light of these estimates, a relatively large number of BHs can be completely removed from their host haloes. In this model, 500 km/s is the critical velocity for ejection of BHs from a static NFW potential of Halo 1, while kick velocities as low as $\sim 300$ km/s can remove BHs at $z = 7$. Halo 2 is more massive and thus less sensitive to gravitational wave recoil. Only a small fraction of highest velocities can eject BHs from static NFW potential where the critical velocity is $v_{\mathrm{kick}} \sim 1350$ km/s and a moderate fraction from a evolving NFW potential. On the other hand, the Einasto profile predicts a lower central density and BHs can easily be removed from their hosts at both high and low redshifts.

Evolution and mass growth of the parent haloes clearly impact their capability to retain recoiling BHs. However, since parameters on which the recoil velocity depends are uncertain, the additional observational constraints on merging or recoiling BHs are needed to determinate the kick velocity distribution more accurately.

The chosen halo mass interval represents hosts of massive field galaxies at redshifts $z < 1$. Fakhouri et al. (2010) used Millennium (Springel et al. 2005) and Millennium II (Boylan-Kolchin et al. 2009) simulations to construct merger trees of DM haloes and quantify their merger rates. These authors have shown that Milky Way-sized halo has, on average, experienced one merger with halo mass ratio > 0.1 since $z = 1$, and seven mergers with the same mass ratio since $z = 7$. Similarly, the host of a massive elliptical galaxy had one merger since $z = 1$ and nine mergers since $z = 7$. At redshift $z = 1$, the static and evolving potentials do not differ significantly. Only BHs with highest velocities can escape host haloes. At higher redshifts, mergers were more common and 40% lower kick velocities are able to eject BHs at redshift $z = 7$, which makes the difference between the static and evolving potential more pronounced. Growth of the SMBH by mergers might be suppressed in an evolving NFW halo potential, while ejections from a static NFW potential would be rare. If the Einasto profile is considered, then a larger number of complete BHs ejections is expected.

Fakhouri et al. (2010) have shown that the halo merger rate (number of mergers per halo per redshift) is nearly independent of redshift for $z < 15$ and that the dependence on halo mass is weak (their Fig. 3, left panel). Having this in mind, the halo mass function can be used for a crude estimate of halo masses whose mergers are most common at each redshift. For example, Halo 1 in this model at $z = 5$ has mass of $\sim 2 \times 10^{10}\,M_\odot$. The halo mass function (Reed et al. 2003, their Fig. 2) shows that at $z = 5$ haloes with masses $\sim 10^{10}\,M_\odot$ are most abundant, and so mergers of these haloes are most common mergers at the given redshift. At the same redshift, haloes with masses $\sim 10^{12}\,M_\odot$ (mass of Halo 1 in static potential) and their mergers would be rare. This implies that BH ejections would be more likely in the evolving potential at high redshifts compared to static potential since mergers of the given halo mass are the most common mergers and critical kick velocity is relatively low. Similarly, Halo 2 at $z = 5$ has mass of $\sim 2 \times 10^{11}\,M_\odot$. Halo mass function given by Reed et al. (2003) predicts high number of similar

mass halo mergers at the given redshift while there are no $2 \times 10^{13} M_\odot$ haloes and thus no their mergers. This could also impact the BH growth in the evolving halo. At lower redshifts, as the DM halo grows in mass, the difference between the static and evolving potential becomes less pronounced.

The considered halo mass interval also corresponds to massive galaxies in proto-clusters at higher redshifts. Haloes that end up in clusters have formed earlier than the isolated haloes of the same mass and they have 3-5 times higher merger rates (Gottlöeber et al. 2001). However, in proto-cluster environment, the density is higher and thus ejected BHs are more likely to settle down in cluster's centre.

Note that this method is approximative for two reasons:

(1) It is assumed that the halo growth is only due to a smooth cold mode accretion. Since the considered haloes have masses that typically hosts massive field galaxies, mergers can be ignored since in low density regions, the accretion from the cosmic web dominates. However, the same mass interval is also typical of the proto-cluster environment. Proto-clusters are early over-densities of massive galaxies and thus, in these regions, merger rates are higher. Mergers would affect the assumed smooth accretion as well as BH trajectories.

(2) Trajectories of recoiling BHs are followed in a pure DM potential. Interactions with stars and gas tend to slow down a recoiling BH and bring it back to the galaxy core after several oscillations (e.g. Merritt et al. 2004, Madau and Quataert 2004, Boylan-Kolchin et al. 2004, Gualandris and Merritt 2008, Blecha et al. 2011, Guedes et al. 2011, Sijacki et al. 2011). Since this model excludes gas, it is assumed that the BH that reaches the galaxy center stays there and further oscillations are ignored. As a consequence of this assumption, BHs in this model either settle back to the galaxy core or completely leave the parent halo and there are very few rogue BHs wondering in the galaxy's halo. In order to get more accurate results, effects of gas should be included.

REFERENCES

Baker, J. G., Boggs, W. D., Centrella, J., Kelly, B. J., McWilliams, S. T., Miller, M. C. and van Meter, J. R.: 2002, *Astrophys. J.*, **668**, 1140.

Baker, J. G., Centrella, J., Choi, D.-I., Koppitz, M., van Meter, J. R. and Miller, M. C.: 2006, *Astrophys. J.*, **653**, L93.

Begelman, M. C., Blandford, R. D. and Rees, M. J.: 1980, *Nature*, **287**, 307.

Blanchet, L., Qusailah, M. S. S. and Will, C. M.: 2005, *Astrophys. J.*, **635**, 508.

Blecha, L. and Loeb, A.: 2008, *Mon. Not. R. Astron. Soc.*, **390**, 1311.

Blecha, L., Cox, T. J., Loeb, A. and Hernquist, L.: 2011, *Mon. Not. R. Astron. Soc.*, **412**, 2154.

Bond, J. R., Cole, S., Efstathiou, G. and Kaiser, N.: 1991, *Astrophys. J.*, **379**, 440.

Boylan-Kolchin, M., Ma, C.-P. and Quataert, E.: 2004, *Astrophys. J.*, **613**, L37.

Boylan-Kolchin, M., Springel, V., White, S. D. M., Jenkins, A. and Lemson, G.: 2009, *Mon. Not. R. Astron. Soc.*, **398**, 1150.

Campanelli, M., Lousto, C., Zlochower, Y. and Merritt, D.: 2007a, *Astrophys. J.*, **659**, L5.

Campanelli, M., Lousto, C. O., Zlochower, Y. and Merritt, D.: 2007b, *Phys. Rev. Lett.*, **98**, 231102.

Cardone, V. F., Piedipalumbo, E. and Tortora, C.: 2005, *Mon. Not. R. Astron. Soc.*, **358**, 1325.

Damour, T. and Gopakumar, A.: 2006, *Phys. Rev. D*, **73**, 124006.

Dekel, A. and Birnboim, Y.: 2006, *Mon. Not. R. Astron. Soc.*, **368**, 2.

Devecchi, B., Rasia, E., Dotti, M., Volonteri, M. and Colpi, M.: 2009, *Mon. Not. R. Astron. Soc.*, **394**, 633.

Dutton, A. A. and Macciò, A. V.: 2014, *Mon. Not. R. Astron. Soc.*, **441**, 3359.

Einasto, J.: 1965, *Trudy Inst. Astrofiz. Alma-Ata*, **5**, 87.

Fall, S. M. and Efstathiou, G.: 1980, *Mon. Not. R. Astron. Soc.*, **193**, 189.

Fakhouri, O., Ma, C. and Boylan-Kolchin, M., 2010, *Mon. Not. R. Astron. Soc.*, **406**, 2267.

Favata, M., Hughes, S. A. and Holz, D. E.: 2004, *Astrophys. J.*, **607**, L5.

Fitchett, M. J. and Detweiler, S. L.: 1984, *Mon. Not. R. Astron. Soc.*, **211**, 933.

Gao, L., Navarro, J. F., Cole, S., Frenk, C. S., White, S. D. M., Springel, V., Jenkins A. and Neto, A. F.: 2008, *Mon. Not. R. Astron. Soc.*, **387**, 536.

Gonzalez, J. A., Hannam, M., Sperhake, U., Brugmann, B. and Husa, S.: 2007a, *Phys. Rev. Lett.*, 98w1101G.

Gonzalez, J. A., Sperhake, U., Brugmann, B., Hannam, M. and Husa, S.: 2007b, *Phys. Rev. Lett.*, 98i1101G.

Gottlöeber, S., Klypin, A. and Kravtsov, A. V.: 2001, *Astrophys. J.*, **546**, 223.

Gualandris, A. and Merritt, D.: 2008, *Astrophys. J.*, **678**, 780.

Guedes, J., Madau, P., Mayer, L. and Callegari, S.: 2011, *Astrophys. J.*, **729**, 125.

Haiman, Z.: 2004, *Astrophys. J.*, **613**, 36.

Hayashi, E. and White, S. D. M.: 2008, *Mon. Not. R. Astron. Soc.*, **388**, 2.

Heger, A., Fryer, C. L., Woosley, S. E., Langer, N. and Hartmann, D. H.: 2003, *Astrophys. J.*, **591**, 288.

Herrmann, F., Hinder, I., Shoemaker, D. and Laguna, P.: 2007, *Astrophys. J.*, **661**, 430.

Jiang, F. and van den Bosch, F. C.: 2014, arXiv:1403.6827

Klypin, A. A., Trujillo-Gomez, S. and Primack, J. R.: 2011, *Astrophys. J.*, **740**, 102.

Koppitz, M., Pollney, D., Reisswig, C., Rezzolla, L., Thornburg, J., Diener, P. and Schnetter, E.: 2007, *Phys. Rev. Lett.*, **99**, 1163.

Libeskind, N. I., Cole, S., Frenk, C. S. and Helly, J. C.: 2006, *Mon. Not. R. Astron. Soc.*, **368**, 1381.

Loeb, A.: 2007, *Phys. Rev. Lett.*, **99**, 1103.

Lousto, C. O. and Zlochower, Y.: 2011, *Phys. Rev. Lett.*, **107**. 1102.

Madau, P. and Quataert, E.: 2004, *Astrophys. J.*, **606**, L17.

Madau, P. and Rees M. J.: 2001, *Astrophys. J.*, **551**, L27.

Merritt, D. and Ekers, R. D.: 2002, *Science*, **297**, 1310.

Merritt, D., Graham, A. W., Moore, B., Diemand, J. and Terzić, B.: 2006, *Astrophys. J.*, **132**, 2685.

Merritt, D., Milosavljević, M., Favata, M., Hughes, S. A. and Holz, D. E.: 2004, *Astrophys. J.*, **607**, L9.

Micic, M.: 2013, *Serb. Astron. J.*, **186**, 1.

Micic, M., Abel, T. and Sigurdsson, S.: 2006, *Mon. Not. R. Astron. Soc.*, **372**, 154.

Micic, M., Holley-Bockelmann, K. and Sigurdsson, S.: 2011, *Mon. Not. R. Astron. Soc.*, **414**, 1127.

Navarro, J. F., Frenk, C. S. and White, S. D. M.: 1997, *Astrophys. J.*, **490**, 493.

Navarro, J. F., Hayashi, E., Power, C., Jenkins, A. R. and Frenk, C. S.: 2004, *Mon. Not. R. Astron. Soc.*, **349**, 1039.

Navarro, J. F., Ludlow, A., Springel, V., Wang, J., Vogelsberger, M., White, S. D. M., Jenkins, A., Frenk, C. S. and Helmi, A.: 2010, *Mon. Not. R. Astron. Soc.*, **402**, 21.

Niemi, S.−M., Heinämäki, P., Nurmi, P. and Saar, E.: 2010, *Mon. Not. R. Astron. Soc.*, **405**, 477.

O'Leary, R. M. and Loeb, A.: 2009, *Mon. Not. R. Astron. Soc.*, **395**, 781.

O'Leary, R. M. and Loeb, A.: 2012, *Mon. Not. R. Astron. Soc.*, **421**, 2737.

Redmount, I. H. and Rees, M. J.: 1989, *Comments on Astrophysics*, **14**, 165.

Reed, D. S., Gardner, J., Quinn, T., Stadel, J., Fardal, M., Lake, G. and Governato, F.: 2003, *Mon. Not. R. Astron. Soc.*, **346**, 565.

Reed, D. S., Koushiappas, S. M. and Gao, L.: 2011, *Mon. Not. R. Astron. Soc.*, **415**, 3177.

Rees, M. J. and Ostriker, J. P.: 1977, *Mon. Not. R. Astron. Soc.*, **179**, 541.

Schnittman, J. D.: 2007, *Astrophys. J.*, **667**, L133.

Schnittman, J. D. and Buonanno, A.: 2007, *Astrophys. J.*, **662**, L63.

Sesana, A.: 2007, *Mon. Not. R. Astron. Soc.*, **382**, L6.

Sijacki, D., Springel, V. and Haehnelt, M. G.: 2011, *Mon. Not. R. Astron. Soc.*, **414**, 3656.

Springel, V. et al.: 2005, Nature, **435**, 629.

Stadel, J., Potter, D., Moore, B., Diemand, J., Madau, P., Zemp, M., Kuhlen, M. and Quilis, V.: 2009, *Mon. Not. R. Astron. Soc.*, **398**, L21.

van den Bosch, F. C., Jiang, F., Hearin, A., Campbell D., Watson, D. and Padmanabhan, N.: 2014, *Mon. Not. R. Astron. Soc.*, **445**, 1713.

Vicari, A., Capuzzo-Dolcetta, R. and Merritt, D.: 2007, *Astrophys. J.*, **662**, 797.

Volonteri, M.: 2007, *Astrophys. J.*, **663**, L5.

Volonteri, M. and Perna, R.: 2005, *Mon. Not. R. Astron. Soc.*, **358**, 913.

Volonteri, M., Gultekin, K. and Dotti, M.: 2010, *Mon. Not. R. Astron. Soc.*, **404**, 2143.

Wise, J. H. and Abel, T.: 2005, *Astrophys. J.*, **629**, 615.

White, S. D. M. and Rees, M. J.: 1978, *Mon. Not. R. Astron. Soc.*, **183**, 341.

Zhao, D. H., Jing, Y. P., Mo, H. J. and Borner, G.: 2009, *Astrophys. J.*, **707**, 354.

Zier, C.: 2005, *Mon. Not. R. Astron. Soc.*, **364**, 583.

# ГРАВИТАЦИОНИ УЗМАК ЦРНИХ РУПА У СТАТИЧКОМ И ЕВОЛУИРАЈУЋЕМ ПОТЕНЦИЈАЛУ ХАЛОА ТАМНЕ МАТЕРИЈЕ

**M. Smole**

*Astronomical Observatory, Volgina 7, 11060 Belgrade 38, Serbia*

E–mail: *msmole@aob.rs*

У овом раду се прате трајекторије црних рупа које услед емисије гравитационих таласа добијају гравитациони узмак и крећу се у статичком и еволуирајућем потенцијалу халоа тамне материје. Испитане су NFW и Einasto расподеле густине. Разматрани халои представљају халое у чијим се центрима налазе масивне, изоловане спиралне и елиптичне галаксије. Испитана је критична брзина коју црне рупе морају добити услед емисије гравитационих таласа како би напустиле хало на различитим црвеним помацима. Нашли смо да је на црвеном помаку $z = 7$ потребна $\sim 40\%$ мања брзина него на црвеном помаку $z = 1$. Највећа разлика између статичког и еволуирајућег потенцијала се примећује близу критичне брзине за избацивање црне рупе и на високим црвеним помацима. Када се упореде NFW и Einasto расподеле густине добија се да су потребне $\sim 30\%$ веће брзине за избацивање црне рупе из халоа тамне материје описаног NFW профилом.